Biochemical Pharmacology 83 (2012) 1183–1194

Contents lists available at SciVerse ScienceDirect

Biochemical Pharmacology

journal homepage: www.elsevier.com/locate/biochempharm

Inhibition of tumor cell growth, proliferation and migration by X-387, a novel active-site inhibitor of mTOR

Si-meng Chen [a], Jia-li Liu [a], Xiang Wang [a], Chris Liang [b], Jian Ding [a,*], Ling-hua Meng [a,*]

[a] Division of Anti-tumor Pharmacology, State Key Laboratory of Drug Research, Shanghai Institute of Materia Medica, Chinese Academy of Sciences, Shanghai 201203, PR China
[b] Xcovery, LLC, West Palm Beach, FL, USA

ARTICLE INFO

Article history:
Received 7 December 2011
Accepted 17 January 2012
Available online 26 January 2012

Keywords:
X-387
mTOR kinase
Cancer therapy
Cell migration
Autophagy

ABSTRACT

The mammalian target of rapamycin (mTOR), is deregulated in about 50% of human malignancies and exists in two complexes: mTORC1 and mTORC2. Rapalogs partially inhibit mTORC1 through allosteric binding to mTORC1 and their efficacy is modest as a cancer therapy. A few mTOR kinase inhibitors that inhibit both mTORC1 and mTORC2 have been reported to possess potent anticancer activities. Herein, we designed and synthesized a series of pyrazolopyrimidine derivatives targeting mTOR kinase domain and X-387 was identified as a promising lead. X-387 selectively inhibited mTOR in an ATP-competitive manner while sparing a panel of kinases from the PIKK family. X-387 blocked mTORC1 and mTORC2-mediacted signaling pathway in cell lines with activated mTOR signaling and in rapamycin-resistant cells. Specifically, X-387 inhibited phosphorylation of AKT at T308, which is thought to be a target of PDK1 but not mTOR. Such activity was not due to inhibition of PI3K since X-387 did not inhibit translocation of AKT to the cell membrane. X-387 induced autophagy as observed for other mTOR inhibitors, while induced autophagy is pro-survival since concurrent inhibition of autophagy by 3-MA reinforced the antiproliferative activity of mTOR inhibitors. X-387 also inhibited cell motility, which is associated with decrease in activity of small GTPases such as RhoA, Rac1 and Cdc42. Taken together, X-387 is a promising compound lead targeting mTOR and with a wide spectrum anticancer activity among tumor cell lines. The data also underscores the complexity of the mTOR signaling pathways which are far from being understood.

1. Introduction

The serine/threonine kinase mTOR (mammalian target of rapamycin) is a critical regulator of cellular metabolism, growth and proliferation and resides in at least two separate complexes: mTORC1 and mTORC2. mTORC1 is composed of mTOR, raptor, mLST8 and deptor [1,2]. mTOR, mLST8 and deptor are also present in mTORC2. Other proteins, i.e. rictor, mSIN1 and PRR5 are found exclusively in mTORC2 [3]. The best-known substrates of mTORC1 are S6 kinases (S6K1 and S6K2) and 4E-BP1, both substrates are involved in protein translation [4]. To coordinate cell growth and proliferation, mTORC1 responds to not only growth factors but also energy, amino acid and oxygen levels, whereas mTORC2 activation is less-defined, but seems to be regulated also by growth factors. mTORC2 has been reported to phosphorylate C-terminal hydrophobic motif of some AGC kinases such as AKT and SGK, leading to their full activation [5].

mTOR pathway is frequently and inappropriately activated in a number of human malignancies as a result of improper activation of receptor tyrosine kinases, PI3K and AKT or inactivation of tumor suppressors such as LKB1, PTEN, or TSC1/2. Moreover, increased level or phosphorylation of downstream targets of mTORC1 has been reported in various human solid tumors and hematopoietic malignancies, in which they correlate with tumor aggressiveness and poor prognosis [6,7]. Studies have shown that genetic alterations that activate mTOR are sensitive to pharmacologic inhibition of mTOR [8,9].

The first generation mTOR inhibitors include the well-known Rapamycin and its analogues including temsirolimus, everolimus and deforolimus. Rapamycin analogues, namely, raplogs have the same molecular scaffold but different physiochemical properties. Rapalogs inhibit mTOR activity through allosteric binding to the FKBP12-rapamycin binding domain of mTORC1. They are identified as cytostatic agents against a number of human cancers. However, allosteric inhibition of mTORC1 by rapalogs seems to be insufficient to achieve broad and robust efficiency in clinic, partially due to the general feedback activation of AKT and ERK/MAPK. Furthermore, phosphorylation of AKT by mTORC2, which is not inhibited by raplogs, is vital for tumor maintenance and progression in a number of solid tumors. Therefore, there is

* Corresponding authors at: Division of Anti-tumor Pharmacology, State Key Laboratory of Drug Research, Shanghai Institute of Materia Medica, Chinese Academy of Sciences, 555 Zu Chong Zhi Road, Zhangjiang Hi-Tech Park, Shanghai 201203, PR China. Fax: +86 21 50806722.
E-mail addresses: jding@mail.shcnc.ac.cn (J. Ding), lhmeng@mail.shcnc.ac.cn (L.-h. Meng).

0006-2952/$ – see front matter © 2012 Elsevier Inc. All rights reserved.
doi:10.1016/j.bcp.2012.01.019

increasing interest in discovering active-site inhibitors of mTOR, which simultaneously inhibit mTORC1 and mTORC2 to achieve better antitumor efficacy. AZD8055, AZD2014, INK128, CC-223 and OSI-027 are recently discovered kinase inhibitors and are currently in clinical trials. Though no clinical result has been reported so far, these kinase inhibitors elicit substantially stronger inhibition of tumor growth than raplogs in preclinical studies [10].

We designed and synthesized a series of pyrazolopyrimidine derivatives and identified X-387 as a novel specific ATP-competitive mTOR kinase inhibitor. X-387 efficiently inhibited cellular signaling of mTORC1 and mTORC2, leading to broad antitumor activities without showing obvious tissue type or gene type selectivity. X-387 arrested cell cycle at G1 phase, inhibited cell growth and induced autophagy in A549 cells. In addition, X-387 inhibited cell migration that is associated with decreased activity of GTPases such as RhoA, Rac1 and Cdc42. Interestingly, X-387 also inhibited phosphorylation of AKT T308, and its induction of autophagy appears to antagonize the antiproliferative activity. This study demonstrated X-387 as a promising compound lead targeting mTOR and shed new light on the mechanism of action of mTOR inhibitors, underscoring the complexity of the mTOR signaling pathway.

2. Materials and methods

2.1. Compounds

X-387 (Fig. 1A) was synthesized with a purity >99% by Xcovery. PP242 and rapamycin were purchased from Sigma (Solon, OH, USA) and 3-methylamphetamine (3-MA) from Santa Cruz Technology (Sana Crus, CA, USA). AZD8055, Ku0063794 and PI103 were purchased from Selleck chemicals (Houston, USA). All compounds were dissolved at 10 mM in dimethylsulfoxide (DMSO) as stock solutions and stored at −20 °C. The compounds were diluted in normal saline before each experiment. The final DMSO concentration did not exceed 0.1% (v/v) and 0.1% DMSO in normal saline was used as a vehicle control.

2.2. Immune-complex kinase assay of mTORC1 and mTORC2

MCF-7 cells were grown to about 50% confluence and harvested. Cells were washed twice with cold phosphate buffered saline (PBS), then extracted with the cytosolic fraction extraction buffer [20 mM Tris–HCl (pH 7.5), 100 mM KCl, 0.25 mM Na_3VO_4, 10 mM NaF, 1 mM

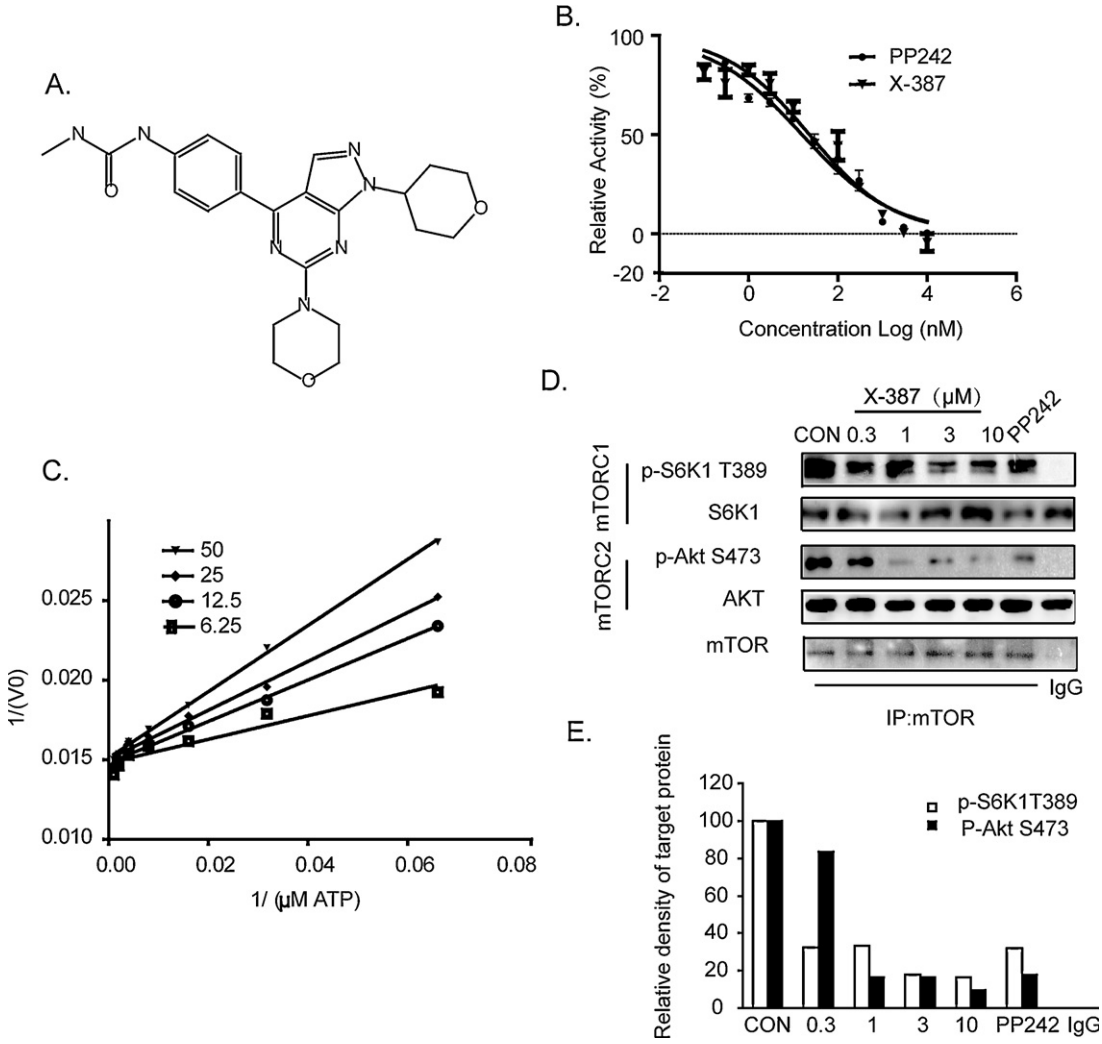

Fig. 1. X-387 is a novel ATP-competitive inhibitor of mTOR. (A) Chemical structure of X-387. (B) Inhibition of mTOR kinase activity by X-387 with the LANCE Ultra mTOR kinase assay. (C) X-387 versus ATP matrix competition. The initial enzyme rate (V0) against 0, 6.25, 12.5, 25, and 50 nM of X-387 at various concentration of ATP was measured to generate the double reciprocal plot. (D) Immuno-complex kinase assay of mTORC1 and mTORC2. Phosphorylation of His-S6K or AKT by immunoprecipitated mTOR complexes was performed. The reaction mixtures were separated and immunoblotted with antibodies against phosphorylated S6K (T389), phosphorylated AKT (S473), S6K1, AKT and mTOR. Lane CON: phosphorylation of AKT or S6K1 in presence of vehicle control (0.1% DMSO); PP242 or X-387: kinase assay in the presence of indicated concentrations of X-387 or PP242 (1 mM). Lane IgG: kinase assay with proteins immunoprecipitated by IgG in presence of vehicle control. (E) Relative phosphorylated S6K1 or AKT in panel D was quantitated and plotted. Data shown are mean ± SD or representative of three independent experiments.

EDTA, 1 mM EGTA, 1% Tween 20, 10% glycerol] containing complete Protease Inhibitor Cocktail (Roche, Switzerland), 1 mM dithiothreitol on ice for 30 min. The cell lysate was centrifuged at 20,000 × *g* at 4 °C for 5 min and the supernatant was collected. One milligram of the cytosolic extract (1 mL) were incubated with 2 μg rabbit IgG (Beyotime Inc, China) or 2.5 μL anti-mTOR (04-385, Millipore, Germany) for 3 h at 4 °C. Protein A + G Agarose (20 μL) was then added and continued to incubate for 2 h. The beads were washed 4 times with 0.5 mL wash buffer (cell extraction buffer supplemented with 50 mM NaCl) and once with the kinase assay buffer (50 mM HEPES, 1 mM EGTA, 0.1% Tween 20, 100 μM ATP, 3 mM $MnCl_2$, 10 mM $MgCl_2$). The immune-complex kinase assay was performed in 50 μL with 500 ng His-AKT1 (14-279, Upstate Biotechnology, USA) or with 500 ng His-S6K peptide and test compounds. The kinase reaction was carried out at 25 °C for 1 h and terminated by adding 10 μL loading buffer (250 mM Tris–HCl, 10% sodium dodecylsulphate, 0.5% bromophenol blue, 50% glycerol, 5% β-mercaptoethanol). The samples were denatured and subjected to Western blot analysis.

2.3. Cell lines and growth inhibition assay

A549 (CCL-185), HCT116 (CCL-247), MCF-7 (HTB22), HL60 (CCL-240), K562 (CCL-243), Molt4 (CRL-1582), Raji (CCL-86), U937 (CRL-1593.2), Wil2-NS (CRL-8155), BT474 (HTB20), H226 (CRL-5826), H23 (CRL-5800), SKOV3 (HTB-77), PC3 (CRL-1435), SGC-7901, H522 (CRL-5810), H1975 (CRL-5908), H460 (HTB-177), H358 (CRL-5807), Calu-3 (HTB-55), and H1650 (CRL-5883) tumor cell lines were obtained from American Type Culture Collection. The gastric cancer cell lines SGC7901, were preserved in our institute. CHO-hIR-EGFP-AKT cells were bought from Amersham Biosciences. Cells seeded in 96-well plate were treated in triplicate with X-387 at 37 °C for 72 h. Cell proliferation was assessed by sulforhodamin B (SRB, Sigma, St. Louis, MO, USA) assay [11]. The IC_{50} values were determined by four-parameter logit method [12]. The following is the model equation where x is the concentration of the compounds in logarithmic form and $F(x)$ would be the response value (antiproliferative rate of a compound at this concentration): $F(x) = ((A - D)/(1 + (x/C)^B))) + D$. The different concentrations and corresponding antiproliferative rates generated a sigmoidal curve, through which IC_{50} were obtained.

CCK8 (cell counting kit 8, Dojindo Laboratories, Japan) assay was performed according to the manufacturer's instructions, which is based on reduction of cellular WST-8 by dehydrogenases to produce an orange colored product. The amount of the formazan dye generated by dehydrogenases in cells is proportional to the number of living cells.

2.4. Kinase assay and immune-complex kinase assay

A GST-tagged truncated human mTOR (animo acid 1360-2549) was expressed and purified as described previously [13]. The kinase activity of the purified truncated mTOR was determined using LANCE® Ultra time-resolved fluorescence resonance energy transfer assay following the manufacturer's instructions. Briefly, mTOR enzyme (20 nM), ATP (100 μM), ULight-4E-BP1 Peptide (25 nM) and test compounds were diluted in kinase buffer (50 mM HEPES pH 7.5, 1 mM EGTA, 3 mM $MnCl_2$, 10 mM $MgCl_2$, 2 mM DTT and 0.01% Tween-20). The reactions were performed in white 384-well Optiplates (PerkinElmer, MA, USA) at room temperature for 2 h and stopped by adding EDTA to 10 mM. Eu-anti-phospho-4E-BP1 (Thr37/46) Antibody (PerkinElmer, MA, USA) was then added to each well to a final concentration of 2 nM. The intensity of the light emission was measured with an EnVision® Multilabel Reader (PerkinElmer, MA, USA) in TR-FRET mode (excitation at 320 nm and emission at 665 nm).

Immuno-complex kinase assay for mTORC1 and mTORC2 was performed as described before [14].

2.5. Western blot analysis

Cells (4.5×10^5) were seeded in six-well plate and exposed to X-387 at indicated concentrations for various times. Cells were harvested and subjected standard Western blot analysis, using antibodies against phosphor-p70S6K1 (9206), phosphor-4E-BP1 (2855), 4E-BP1 (9132), phosphor-TSC2 (3617), phosphor-GSK-3β (9323), GSK-3β(9315), c-Myc (9402), LC3 A/B (4108) and phosphor-AKT (9271) (Cell Signaling Technologies, Cambridge, MA), Cyclin D1 (sc-717), and GAPDH (sc-47724) antibody (Santa Cruz Biotechnology, Santa Cruz, CA).

2.6. FACs analysis

Cells exposure to X-387 for 24 h were harvested for FACS analysis as described previously [15]. Histograms of FSC-H were collected as the parameter for relative cell size.

2.7. AKT translocation assay

CHO-hIR cells [16] stably expressing AKT1-EGFP were seeded at a density of 5×10^3 in a 96-well black plate (Greiner Bio-One). Cells were incubated in serum-free media for 24 h followed by treatment of compounds for 1 h. After addition of IGF-1 (250 ng/mL) for 10 min, the cells were fixed with 4% paraformaldehyde for 10 min at room temperature. The fluorescent images were captured with a fluorescence microscope (BX51; Olympus, Tokyo, Japan).

2.8. Wound-healing assay

Wound-healing assays were conducted as described previously [17].

2.9. Cell migration assay

Cell migration was evaluated using an 8-mm pore size Transwell system (Costar, Corning, NY). Medium containing 10% FBS was added to the lower chambers and cells were suspended in serum-free medium containing indicated compounds and added to the upper chambers. Cells migrated to the lower chamber were detected and quantitated as described previously [17]

2.10. Pull-down analysis of Rho A, Rac1 and Cdc42

Quantification of GTP-bound Rho A, Rac1 and Cdc42 was performed using the BK124, BK128 and BK127 G-LISA assay as instructed by the manufacturer (Cytoskeleton, Denver, USA). Briefly, MNK-45 cells after treatment were suspended in lysis buffer. Cell extracts were incubated in separate wells of the G-LISA plate. The wells were probed with anti-Rho A, Rac1 or Cdc42 monoclonal antibodies and a secondary antibody. Finally, the plate was developed with a colorimetric substrate and the absorbance was read at 490 nm with a multiwall plate reader.

2.11. Statistical analysis

Data were presented as mean ± SD from at least three independent experiments and differences were considered significant when $P < 0.05$ as determined by Student's t test.

3. Results

3.1. X-387 is a potent, specific and ATP-competitive inhibitor of mTORC1 and mTORC2

In an effort to discover new mTOR active site inhibitors, high throughput screening was carried out using LANCE mTOR kinase

assay. X-387 was found to potently inhibit the kinase activity of mTOR among a series of pyrazolopyrimidine derivatives (Fig. 1A). As X-387 possesses new chemical structure that is different from the chemicals undergoing preclinical trials currently, it has been selected for further study. By measuring phosphorylation of 4E-BP1 at Thr37/46, X-387 inhibited the kinase activity of recombinant mTOR kinase domain with an IC_{50} of 23.2 nM (Fig. 1B). X-387 is >10-fold more potent against mTOR than class I PI3K isoforms in

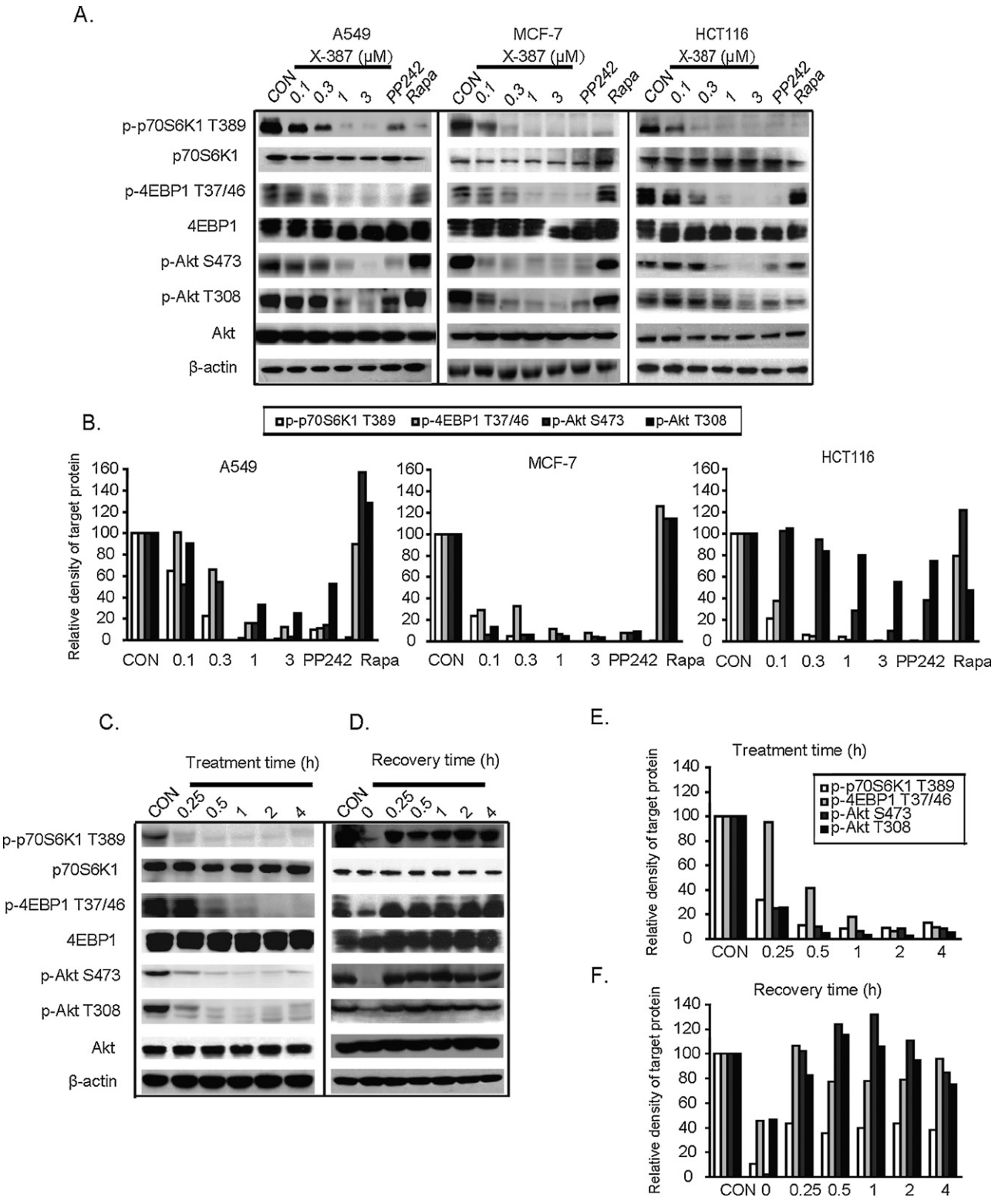

Fig. 2. X-387 suppresses downstream signaling mediated by mTORC1 and mTORC2 in tumor cells. (A) A549, MCF-7 and HCT116 cells cultured in the presence of 10% fetal bovine serum were treated by PP242 (1 μM), Rapamycin (10 nM) or X-387 at indicated concentrations for 1 h. (C) A549 cells were exposed to X-387 (3 μM) for different times. (D) After treatment with 3 μM X-387 for 1 h, A549 cells were further incubated in drug-free medium for the indicated times. Western blot analysis was conducted with antibodies against indicated proteins. (B) (E) and (F): Relative phosphorylated S6K1, 4EBP1 or AKT in panel A, C and D was quantitated and plotted. Data shown are representative of three independent experiments.

Ambit binding assays (Supplemental Table 1). X-387 was further counter screened against other lipid kinases in the Invitrogen Adapta assay and displayed <50% inhibition at 1 μM against PI4K alpha, PI4K beta, PI3K-C2 alpha, PI3K-C2 beta, hVPS34, SPHK1 and SPHK2 (data not shown). We next determined the effect of X-387 on the activity of DNA-PK, ATM and ATR, which belong to the PIKK family and are required for the phosphorylation of H2AX upon DNA strand breaks induced by camptothecin (CPT). By measuring the level of phosphorylated (γ-H2AX), we found X-387 did not inhibit CPT-induced ATM, ATR and DNA-PK activation even at 3 μM (Supplemental Fig. 1). Therefore, X-387 is highly selective against mTOR among the kinases tested.

As X-387 was designed to inhibit the catalytic activity of mTOR and molecular modeling based on the structure adapted from the PI3Kγ crystal structure suggested that X-387 interacted with a few critical residues within the kinase catalytic domain (Supplemental Fig. 2). A representative ATP matrix assay with X-387 was performed. As shown in Fig. 1C, double–reciprocal plots of the initial reaction rate versus ATP concentration showed typical competitive inhibition. These results strongly suggested that X-387 functions as an active site inhibitor of mTOR in an ATP-dependent manner.

To test the activity of X-387 against the catalytic activity of cellular mTORC1 and mTORC2, the complexes were immunoprecipitated from MCF-7 cells with anti-mTOR antibody. As S6K1 and AKT are specific substrates for mTORC1 or mTORC2 respectively [18], mTORC1 and mTORC2 kinase reactions were performed with their respective substrates. Both X-387 and PP242, a reported selective mTOR kinase inhibitor [19], efficiently blocked mTORC1-mediated phosphorylation of p70S6K at T389 and mTORC2-mediated phosphorylation of AKT at S473 in a concentration-dependent manner (Fig. 1D) [18]. The relative phosphorylated S6K1 and AKT compared with respective control group (Lane CON) were quantitated and plotted in Fig. 1E.

Therefore, X-387 is a highly selective, ATP competitive inhibitor against mTOR and inhibits the kinase activity of both mTORC1 and mTORC2.

3.2. Inhibition of mTOR signaling in PI3K/mTOR hyper-activated tumor cells by X-387

We next investigated the effect of X-387 on mTORC1- and mTORC2-mediated signaling in human tumor cells. Three cell lines with hyper-activated mTOR signaling were selected for investigation: human non-small cell lung cancer A549 cells with LKB1 loss and KRAS mutation, human breast cancer MCF-7 cells with PI3K mutation and p70S6K1 amplification and human colon cancer HCT116 cells with PI3KCA H1047R mutation and KRAS mutation.

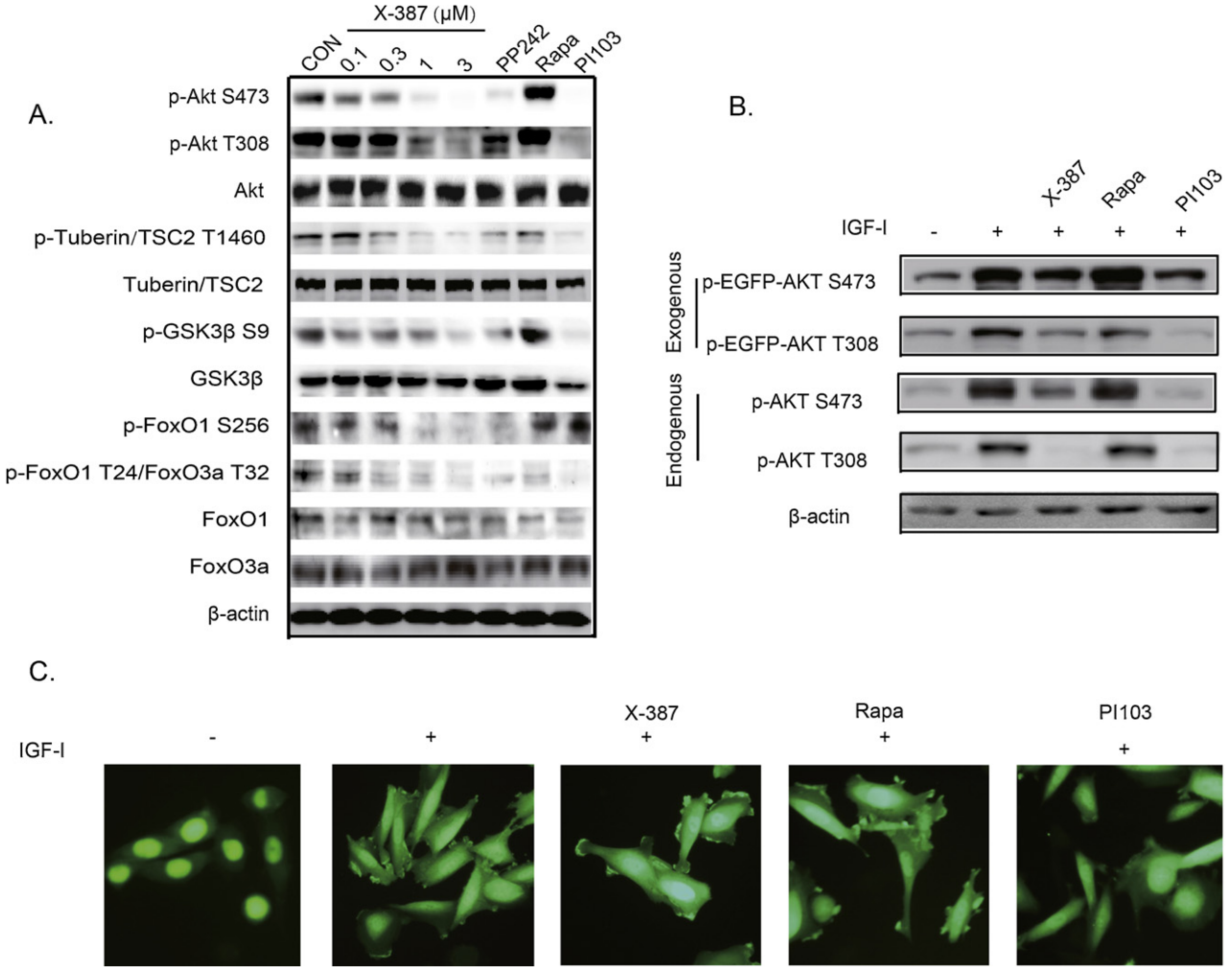

Fig. 3. X-387 inhibits AKT activity without affecting translocation of AKT to membrane stimulated by IGF. (A) A549 cells were treated with various concentrations of X-387, PP242 (1 μM), Rapamycin (10 nM), PI103 (1 μM) for 1 h. Phosphorylated AKT and its representative substrates were detected by Western blot. (B and C) Serum-deprived CHO-EGFP-AKT cells were pre-incubated with X-387 (3 μM), Rapamycin (10 nM), PI103 (1 μM) for 1 h followed by stimulation of IGF-1 (250 ng/mL) for 10 min. Phosphorylated both exogenous (EGFP-AKT) and endogenous AKT at S473 and T308 were analyzed by Western blot (B). The green fluorescence indicating EGFP-AKT fusion protein was captured with the inverted fluorescent microscopy (C). Representative images from three independent experiments are presented.

mTORC1 has been reported to phosphorylate 4E-BP1 at Thr37/Thr46 and possibly Ser65 and Thr70 as well as S6K1 at Thr389 [20]. In spite of different driving forces activating mTORC1 signaling in tested cell lines, phosphorylation of p70S6K1 at T389 and 4EBP1 at T37/46 were all inhibited by X-387 in a concentration-dependent manner. Treatment with 0.1 μM X-387 for 1 h resulted in decreased phosphorylated p70S6K1 and 4E-BP1 by 40–70% and X-387 at 3 μM completely abolished mTORC1-mediated cellular signaling (Fig. 2A and B). In contrast, rapamycin potently inhibited phosphorylation of p70S6K1, but was much less effective in inhibiting 4E-BP1 at T37/46. X-387 also inhibited phosphorylation of AKT at S473, while rapamycin activated the phosphorylation at this residue through the well-known feedback mechanism [21]. Surprisingly, X-387 also inhibited phosphorylation of AKT at T308 (Fig. 2A) and the possible mechanism will be explored later. We also detected cellular signaling in non-malignant HMEC and MCF-10A cells after X-387 treatment. Though mTOR is not highly activated in these cells, X-387 as well as PP242 inhibited mTORC1 and mTORC2 signaling in these cells, suggesting mTOR inhibitors inhibited mTOR signaling irrespective the active status of mTOR (Supplemental Fig. S3). However, the effect on cellular function such as growth and proliferation might be different, which deserves further investigation.

We next detected the time response of mTOR signaling in A549 cells upon X-387 treatment. Both mTORC1 and mTORC2 were readily inhibited within 15 min after treated with X-387 at 3 μM and this effect persisted up to 4 h (Fig. 2B, C and E). To test whether the effect of X-387 on mTOR signaling is reversible, A549 cells were incubated in drug-free medium for indicated times after treatment with X-387 for 1 h. As shown in Fig. 2D and F, phosphorylated p70S6K1, 4E-BP1 and AKT recovered to the level comparable to that in control group within 15 min after X-387 removal, indicating the action of X-387 on mTOR is rapidly reversible, suggesting that continuous inhibition of mTOR may be required for efficacy [19].

3.3. X-387 inhibits AKT activity and blocks phosphorylation of AKT at T308

AKT enhances cellular survival through phosphorylation of a large number of substrates including FoxO1, GSK3, BAD, TSC2, ASK1, $p27^{Kip1}$ and IKKα etc. [22]. As genetic knockout of mTORC2 impairs AKT phosphorylation and function [5], we investigated the effect of X-387 on the phosphorylation of a subset of AKT substrates including TSC2 at T1460, FoxO1 at S256 and T24, FoxO3a at T32 and GSK3β at S9. As shown in Fig. 3, phosphorylated TSC2, FoxO1, FoxO3a and GSK3β decreased in a concentration-dependent manner in the presence of X-387, while phosphorylation of these proteins increased or at least remained unchanged upon rapamycin treatment. These results indicated that X-387 inhibited the downstream signaling of AKT, while rapamycin was unable to elicit this effect, suggesting the critical role of mTORC2 in maintaining downstream signaling of AKT.

We interestingly found that X-387 also inhibited phosphorylation of AKT at T308 (Fig. 2). We sought to explore whether inhibition of phosphorylation AKT at T308 by X-387 is due to its off target effect against PI3K. AKT is recruited by PIP3 to cellular membrane and then phosphorylated by PDK1 at T308 after IGF stimulation. A CHO-hIR cell line stably expressing EGFP-AKT fusion protein [16] was utilized to determine the location of AKT after X-387 treatment. Consistent with the observation in tumor cells, X-387 inhibited both endogenous (native AKT in cells, ~60KD) and exogenous AKT (EGFP-AKT fusion protein, ~90KD) phosphorylation at S473 and T308 (Fig. 3B). AKT was found to localize in cytoplasm and nucleus after serum deprivation, while activation of PI3K by IGF resulted in the translocation of AKT to the cellular membrane, which was demonstrated as the fluorescent foci on the membrane (Fig. 3C). Treatment of cells with a PI3K/mTOR dual inhibitor PI103 abrogated the redistribution of AKT, while rapamycin failed to inhibit this process. Although X-387 inhibited phosphorylation of AKT at both S473 and T308, X-387 failed to prevent the translocation of AKT to membrane, indicating that decreased phosphorylation at T308 is not due to inhibition of PI3K. It has been reported that PP242 had no effect on phosphorylation of AKT at T308 in cells transected with AKT S473D mutant, though it did inhibit pT308 in cells with wild type AKT [19]. These results suggested that inhibition of phosphorylation of AKT at T308 might be due to defect in phosphorylation at S473 by mTORC2 after X-387 treatment.

3.4. X-387 displays significant antiproliferative activity in a broad range of human tumor cells

As mTOR displays a critical role in cell growth and proliferation, we tested the antitumor activity of X-387 in a panel of tumor cells originated from different tissue types. As shown in Fig. 4A, X-387 elicited profound growth suppression with IC_{50} values generally in the submicromolar range, even in the rapamycin-resistant HCT116 cells.

The constitutive activation of the mTORC1 pathway is detectable in almost all NSCLC (non-small cell lung cancer) patient samples, suggesting the potential of using mTOR inhibitors as therapeutic agents in these tumors. However, the therapeutic efficacy of rapalogs seems modest, at least as monotherapy [23]. To further elucidate whether X-387 has improved antiproliferative activity against NSCLC cells comparing to rapamycin, their anti-proliferative activities were tested in nine representative NSCLC cell lines. These cell lines harbor diverse gene mutations responsible for mTOR activation, such as PI3KCA activation/mutation, PTEN inactivation, EGFR deregulations and RAS mutation (Fig. 4B). The IC_{50}s of X-387 in these cell lines were depicted in Fig. 4B. Despite the different genotype contexts, X-387 consistently inhibited cell proliferation with IC_{50} ranging from 0.2 to 1.6 μM. By comparing the relative proliferation rates in the presence of 1 mM rapamycin or 3 mM of X-387 in these cell lines (Fig. 4B, lower panel), we found that the antiproliferative effect of rapamycin is highly variable. For example, rapamycin barely inhibited the proliferation of H460 cells at the concentration of 1 μM, while it displayed significant activity against H1975 cells.

We extended the test scope of X-387 to National Cancer Institute 60 cell lines (NCI-60). X-387 displayed potent growth inhibition in the cell lines with GI_{50}s (the concentration of a chemical which inhibits cell growth by 50%) ranging from 37 nM to 1.8 μM, which further demonstrated that X-387 possessed a board spectrum of antitumor activity without obvious cell type selectivity (Fig. 4C). Interestingly, the LC_{50}s (the concentration of a chemical which kills 50% of cells) of X-387 against NCI-60 were mostly above 100 μM (data not shown), which are much greater than its GI_{50}s, indicating that the anticancer activity induced by X-387 are likely due to growth or proliferation arrest instead of cell death.

3.5. X-387 induces cell cycle arrest and cell size reduction

mTOR is an important factor involved in regulating cell growth and G1-S phase transition. Data obtained from NCI60 screening indicated that X-387 likely exerts its anticancer activity via inhibiting cell growth or inducing proliferation

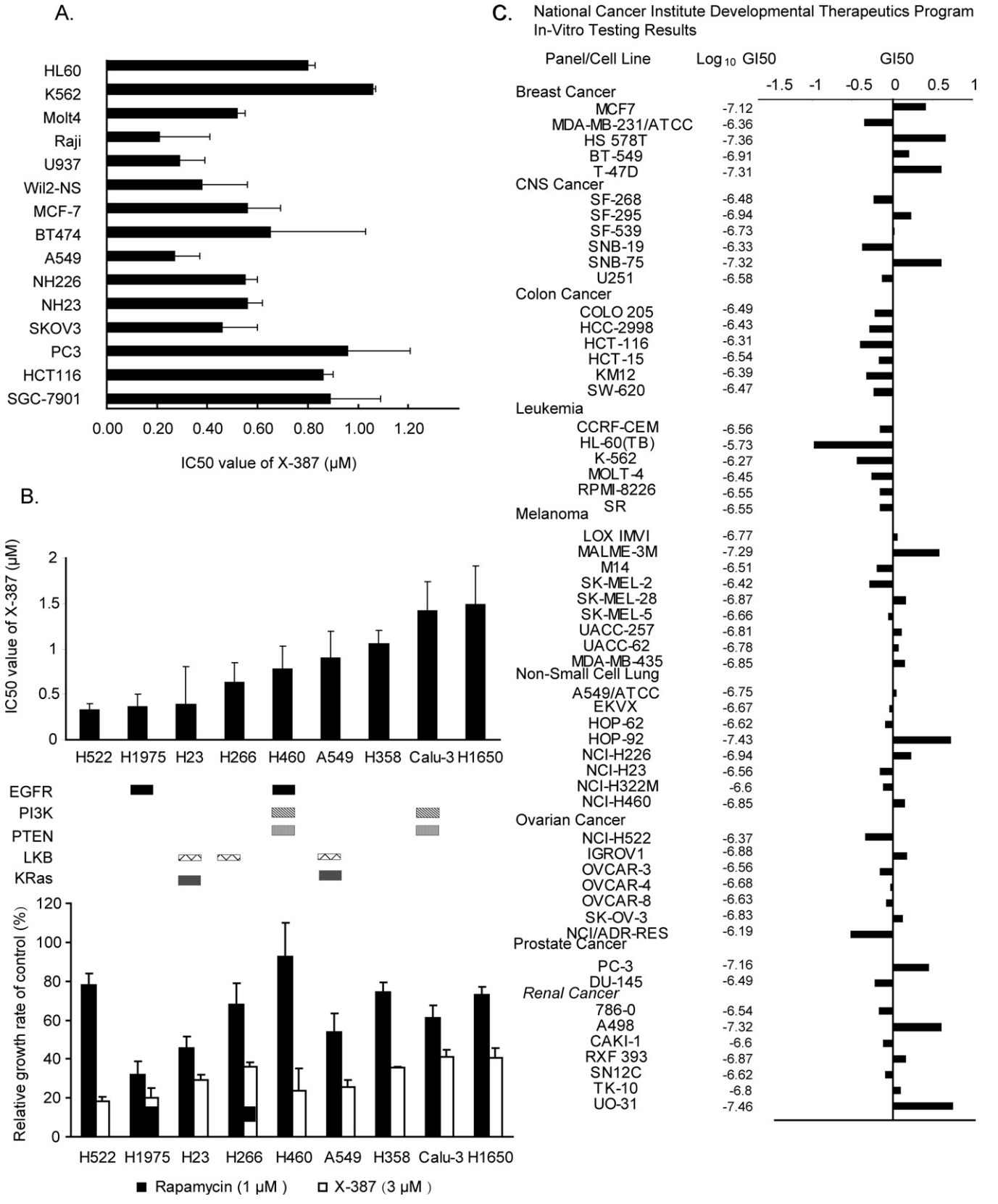

Fig. 4. X-387 possesses potent antiproliferative activity in a wide panel of cancer cells. (A) Antiproliferative activity of X-387 against a panel of tumor cell lines originated from different tissue types was determined by the sulforhodamine B (SRB) or MTT assay after 72 h treatment. IC50s plotted as mean ± SD (μM) were from three separate experiments. (B) Antiproliferative activity of X-387 or rapamycin in a panel of nine NSCLC cell lines was determined by SRB assay after 72 h treatment. IC50s of X-387 (upper panel) or relative cell proliferation (lower panel) in the presence of both X-387 (3 μM) and rapamycin (1 μM) were plotted as mean ± SD from three separate experiments. EGFR: cell lines with EGFR mutation or over-expression; PI3K: cell lines with PI3K mutation or over-expression; LKB1: cell lines with loss of function of LKB1; RAS: cell lines with over activation of RAS. (C) The antitumor activity of X-387 in NCI-60 screen. X-387 was submitted to National Cancer Institute Developmental Drug Program (NCI, DTP) for NCI-60 screen with a designed ID NSC756053 (http://dtp.nci.nih.gov/webdata.html). The mean graph for GI50s of X-387 against NCI 60 cell lines was produced by computer processing of the GI50s. The graph is centered to the arithmetic mean of the −log GI50s for all cell line responses. Bars to the left represent delta values for the most resistant cell lines while these projecting to the right indicate the most sensitive cell lines.

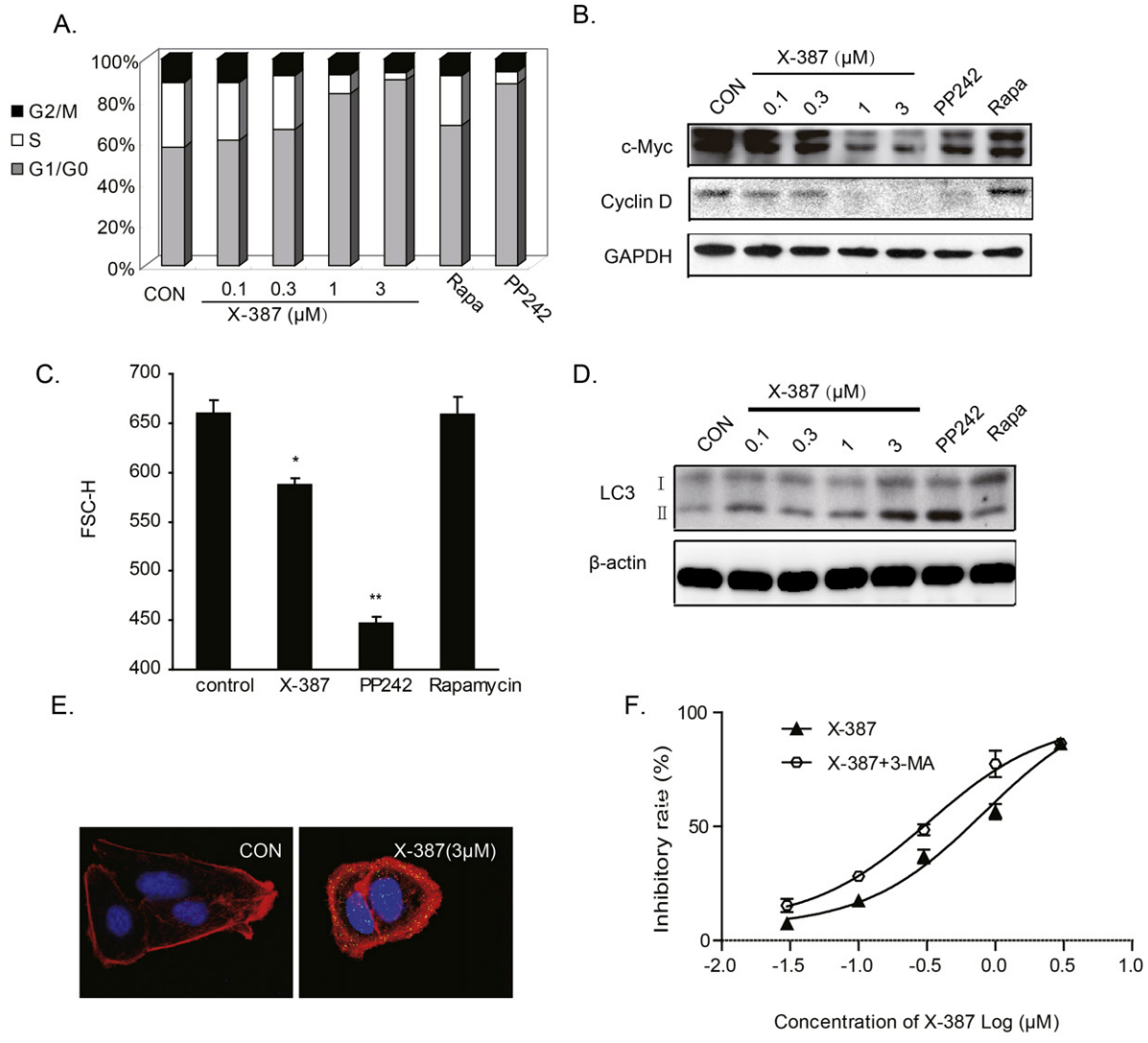

J.

compounds	X-387	X-387 + 3-MA	PP242	PP242 + 3-MA	Ku0063794	Ku0063794 + 3-MA	AZD8055	AZD8055 + 3-MA
IC50 (nM)	1051 ± 13	344 ± 27	431.9 ± 18	204.3 ± 19	1236 ± 9	689.3 ± 14	63.4 ± 13	31.8 ± 7

Fig. 5. X-387 induces G1 phase arrest, cell size reduction and autophagy in A549 cells. (A and B) Induction of G1 phase arrest by X-387. A549 cells were treated with increasing concentrations of X-387, PP242 (1 μM) or rapamycin (10 nM) for 24 h. DNA content was measured with FACS analysis and protein levels of c-Myc and Cycline D were detected by Western blot. (C) Reduction of cell size by X-387. A549 cells were treated with X-387 (3 μM), PP242 (1 μM) and rapamycin (10 nM) for 48 h and cell size was measured by flow cytometry. (D and E) Induction of autophagy by X-387. (D) Expression of LC3 (LC3-I and LC3-II) was determined by immunoblotting after A549 cells were exposed to different concentrations of X-387, rapamycin (10 nM) or PP242 (1 μM) for 24 h. (E) Cellular distribution of LC-3 after treatment with X-387 (3 μM) for 4 h F-actin was stained with Alexa Fluor ® 635 phalloidin (red fluorescence) and LC-3 was stained anti-LC-3 antibody (green fluorescence). (F) Inhibiting autophagy by 3-MA enhanced the antiproliferative activity of X-387. (J) 3-MA reinforced the antitumor activity of mTOR kinase inhibitors. A549 cells were treated with mTOR kinase inhibitor alone or together with 3-MA (50 μM) for 72 h and antiproliferative activity was determined by SRB assay. Data shown are mean ± SD or representative of three independent experiments.

arrest. We further studied its mechanism of action. A549 cells were treated with various concentrations of X-387 for 24 h and cell cycle distribution was measured. As shown in Fig. 5A, the proportion of A549 cells in the G0-G1 phase significantly increased accompanied with decreased cell population in S phase after X-387 treatment. Consistent with its antiproliferative activity presented in Fig. 4B, X-387 elicited a more profound cell cycle arrest than rapamycin. Consistently, expression of the highly oncogenic proteins known to regulate cell cycle transition, e.g. c-Myc, Cyclin D, was markedly reduced after same treatment (Fig. 5B).

To test the effect of X-387 on cell growth, we measured the relative cell size of A549 cells after treatment with X-387 for 24 h. The cell size (mean FSC-H) of X-387-treated A549 cells was significantly decreased (being about 87% of that in control group), while rapamycin treatment had no significant effect on cell size (Fig. 5C). S6K1 has been implicated in controlling cell size independently of 4E-BP1 in mammalian cells [24]. In the present study, though both rapamycin and X-387 inhibited phosphorylation of S6K1 in A549 cells (Fig. 2), X-387 was more potent in reducing the cell size, suggesting that suppression of cell growth by X-387 may not mediated exclusively by S6K1.

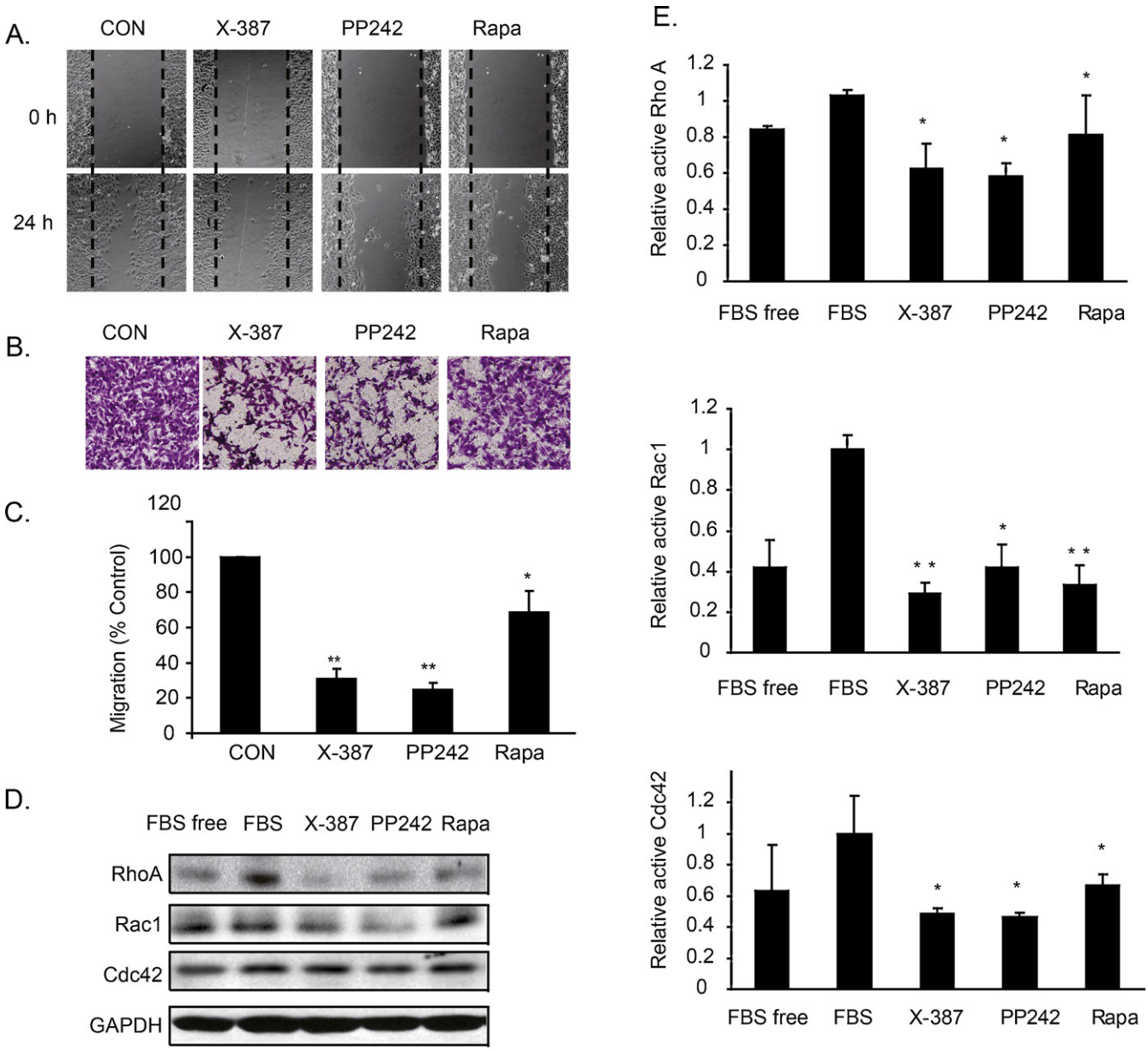

Fig. 6. X-387 inhibits the migration of A549 cells. (A) Migration of A549 cells was detected by wound healing assay after treated with X-387 (3 μM), rapamycin (10 nM) or PP242 (1 μM) for 24 h. Representative images from at least three independent experiments were shown. (B and C) Motility of A549 cells in the presence of X-387 (3 μM), rapamycin (10 nM), or PP-242 (100 nM) was determined by the classic Transwell assay as described in Materials and Methods. Cells invading to the lower aspect of the Boyden chamber filter after 24 h were stained and photographed. (B) Representative images from at least three independent experiments. (C) Quantitative analysis of cell migration. Columns, mean of three experiments; bars, SD. $^{*}P < 0.05$, $^{**}P < 0.01$, difference with vehicle control group. (C) Protein levels of RhoA, Rac1 and Cdc42 were detected by Western blot after A549 cells were treated with X-387 (3 μM), rapamycin (10 nM) and PP242 (1 μM) for 24 h. (D) Down regulation of the active form of RhoA, Rac1 and Cdc42. Cells treated with X-387 (3 μM), rapamycin (10 nM) and PP242 (1 μM) for 24 h were harvested to detect the GTP-bound RhoA (upper panel), Rac1(middle panel) and Cdc42 (lower panel) according to the manufacturer's instructions. Data shown are mean ± SD from three independent experiments. $^{*}P < 0.05$, $^{**}P < 0.01$, difference with the vehicle control group.

3.6. X-387 induces autophagy that attenuates X-387 antitumor activity

It has been reported that both rapamycin and mTOR kinase inhibitors are able to induce autophagy [25], but this effect on their antiproliferative activity is unknown. As shown in Fig. 5D, X-387 induced autophagy as evidenced by increased levels of LC3-II in a dose-dependent manner. Autophagy can also be visualized as the presence of LC3 in autophagosomes, which were detected by immunostaining with antibodies against LC3 after X-387 treatment (Fig. 5E).

Autophagy can be involved either in a pro-survival or pro-death mechanism depending on the circumstances [26]. To test the effect of autophagy on the antiproliferative activity of X-387, cells were co-treated with 3-methyladenine (3-MA, an inhibitor of autophagy) and X-387. As shown in Fig. 5F, 3-MA sensitized X-387-induced inhibition in proliferation with IC_{50} decreased from 1.05 μM to 0.34 μM, indicating that autophagy induced by X-387 is more likely a pro-survival mechanism and simultaneous inhibition of autophagy may enhance X-387's antitumor activity. To further confirm whether this synergetic action is shared by other mTOR kinase inhibitors, we co-treated A549 cells with some published mTOR inhibitors, i.e. AZD8055, PP242 or Ku0063794 and 3-MA. 3-MA enhanced the antitumor activities of all the mTOR inhibitors tested (Fig. 5J), which indicated that inhibiting autophagy induced by mTOR inhibitors may potentiate their anticancer activity.

3.7. X-387 significantly inhibits cell motility through inhibiting cellular GTPase activity of RhoA, Rac1 and Cdc42

Rapamycin have been reported to inhibit cell motility [27–29], suggesting that mTORC1 is involved in the cell migration. Moreover, mTORC2 is reported to regulate actin polymerization and cell polarity during the process of cell migration [30–32]. We thus compared the effect and mechanism of X-387 and rapamycin on cell migration. A wound-healing assay was performed and representative images were shown in Fig. 6A. Both X-387 and rapamycin substantially inhibited migration of A549 cells. A more quantitative Transwell assay was carried out to compare the activity of rapamycin and X-387 against cell migration (Fig. 6B). X-387 inhibited the migration of A549 cells with an inhibitory rate about 70%, which is comparable to that in the presence another mTOR kinase inhibitor PP242 but much higher than that induced by rapamycin (about 30%, Fig. 6C). To exclude the possibility that the inhibitory effect of X-387 on cell migration is due to its activity against cell viability, CCK8 assays were conducted with A549 cells treated by the indicated concentrations of X-387 for 24 h and greater than 95% of the cells were viable after treatment (data not shown). These findings suggest that X-387 more significantly inhibited cell motility than rapamycin probably due to the inactivation of mTORC2 and more complete inhibition of mTORC1.

The Rho family of small GTPases, in particular Rac1, Cdc42 and RhoA, are molecular switches that control the organization and dynamics of the actin cytoskeleton. It has been recently reported that rapamycin inhibits cytoskeleton reorganization and cell motility stimulated by IGF-1 via suppressing RhoA expression and activity [28]. We detected the effect of X-387 on the expression and active form of Rac1, Cdc42 and RhoA in A549 cells. As shown in Fig. 6D, mTOR kinase inhibitors X-387 and PP242 treatment reduced the expression of RhoA and Rac1 with no obvious effect on Cdc42. Rapamycin treatment decreased the expression of RhoA, while sparing the other two GTPases tested. We next examined the active form of RhoA, Rac1 and Cdc42 upon inhibition of mTOR using a pull-down assay that specifically recognizes the active GTP-bound forms. As shown in Fig. 6E, serum stimulation increased activity of RhoA, Rac1 and Cdc42 within 10 min. Pretreatment of X-387, rapamycin or PP242 significantly attenuated the activation of the three GTPases. Consistent with results presented in panels B and C, X-387 and PP242 displayed superior activity than rapamycin in inhibiting the activity of these GTPases.

Collectively, X-387 displayed superior activity than rapamycin in inhibiting cell migration of A549 cells, which is probably due to complete inhibition of mTORC1 as well as mTORC2 is associated with down regulation of the expression and activity of GTPases. The detailed mechanism deserves further investigation.

4. Discussion

The present study described X-387, a novel pyrazolopyrimidine as a potent, selective and ATP-competitive mTOR kinase inhibitor. X-387 attenuated mTOR signaling in human tumor cells and displayed broad anti-proliferative activity. We provided evidence that X-387 inhibited phosphorylation of AKT at T308, without inhibiting the translocation of AKT to the membrane. X-387 induced autophagy, which is pro-survival since concurrent inhibition of autophagy potentiated the anti-proliferative activity of X-387. We also found that X-387 inhibited cell motility, resulted from decreased expression and activity of small GTPases such as RhoA, Rac1 and Cdc42. Taken together, these results suggests that X-387 is a promising mTOR kinase inhibitor with interesting but significant pharmacological effects.

Rapamycin, as a classic allosteric mTOR inhibitor, inhibits mTORC1 but not mTORC2. X-387 was designed and synthesized as a kinase inhibitor interacting with the active site of mTOR as supported by the following data. Firstly, X-387 inhibited the kinase activity of a recombinant mTOR kinase domain, as well as mTORC1 and mTORC2 immunoprecipitated from cells, while sparing other members of the PIKK family in the similar concentration range. Secondly, X-387 acted against mTOR in an ATP-dependent manner. And lastly, molecular docking analysis illustrated that X-387 potentially interact with the ATP-binding pocket of mTOR. Consequently, X-387 inhibited mTOR1- and mTOR2-mediacted cell signaling in various tumor cell lines, whereas rapamycin only partially inhibited the activity of mTORC1 and had no effect on mTORC2.

As a result of the well-known feedback loop between mTORC1 and insulin receptor substrate 1 (IRS-1), treatment with rapalogs in some cases results in elevated AKT activity. mTOR kinase inhibitors inhibited phosphorylation of AKT at Ser473. Interestingly, several mTOR kinase inhibitors were reported to inhibit the phosphorylation of AKT at T308 as well [19,33]. Some compounds, however, inhibited phosphorylation of AKT Thr308 only at relatively high concentrations [14]. Though X-387 possesses distinct structure from Ku-0063794 and PP242, X-387 significantly inhibited AKT phosphorylation at both sites and down-regulated the activity of AKT. It has been demonstrated that inhibition of phosphorylation at T308 is dependent on dephosphorylation of S473 as a result from TORC2 inhibition using sin-knockout cells or cells transfected with AKT S473D mutant [33]. We found that X-387 treatment failed to block translocation of AKT to cellular membrane upon IGF stimulation, while it inhibited AKT phosphorylation at S473 and T308 in CHO-hIR cells expressing EGEP-AKT fused protein, indicating that blockade of phosphorylation of AKT T308 was not due to direct or indirect action of X-387 against PI3K. The exact mechanism is still unclear and X-387 could be a useful tool compound for further study. This study also provided a simple method to determine a compound's selectivity against PI3K or mTORC2 at cellular level by determining the cellular distribution of AKT.

Frequent hyper-activation of AKT and mTOR were found in 51% of NSCLC patient samples and in 74% of NSCLC cell lines [34]. Clinical trials have been conducted to define the efficacy of rapalogs in NSCLC, but unsatisfactory outcomes have been reported with temsirolimus [35]. As an active site inhibitor, X-387 possessed broad antiproliferative activity in a panel of 9 NSCLC cell lines with IC_{50}s ranging from submicromolar to single digit micromolar. Meanwhile, rapamycin displayed activity in very few cell lines, which is consistent with rapalogs' highly variable efficacy in clinic. X-387 also exhibited potent activity against a panel of in-house tumor cell lines as well as the NCI60 panel. Because of its wide spectrum activity against tumor cell proliferation, X-387 may potentially achieve better efficacy compared to rapalogs.

The broad activity of X-387 in tumor cell lines indicated the critical role of mTOR in cell growth and proliferation. Accordingly, we found that X-387 inhibited cell growth and arrested cells in G1 phase without induction of apoptosis in A549 cells. mTOR is also a key factor involved in regulation of autophagy [36] and inhibition of mTOR by X-387 induced autophagy in A549 cells. Autophagy represents an important cell-physiologic response that can be strongly induced in certain states of cellular stress, such as nutrient deficiency. It has been reported that inactivation of autophagy machinery exhibits increasing susceptibility to cancer, i.e. induction of autophagy appears to be a barrier to tumorigenesis [37]. Autophagy is also thought to have prosurvival effects in cells experiencing metabolic and nutritional stress within established tumors, enabling them to escape from apoptosis [38,39]. Therefore, autophagy seems to be double faced in tumor progression and therapy. We found that autophagy provided a prosurvival

mechanism upon X-387 treatment, as concurrent inhibition of autophagy enhanced the antiproliferative activity of X-387. Similarly, Mirzoeva et al. reported that suppression of autophagy promoted PI3K/mTOR dual inhibitor XL765-induced cell death as this manuscript was in preparation [40]. It has also been reported that AZD8055 antagonized chemotherapy-induced cell death through autophagy induction and down-regulation of p62/sequestosome [41]. These results together with our data indicated that inhibition of autophagy would potentiate the antitumor activity of mTOR kinase inhibitors but how autophagy would enable cancer cells to survive upon inhibition of mTOR and whether inhibition of autophagy would improve mTOR inhibitor-based cancer therapy deserves further investigation.

It has been reported that rapamycin inhibited cell motility, indicating the role of mTORC1 in cell motility [28]. mTORC2 has also been reported to control the actin cytoskeleton in a rapamycin-insensitive manner [30]. However, the effect of mTOR kinase inhibitors on cell motility remains unclear. We provided evidence that X-387 more potently attenuated cell motility than rapamycin in A549 cells, which correlated with decreased activity of small GTPases (RhoA, Cdc42 and Rac1). Thus, the effect of X-387 on cell motility might reflect the combined inhibition of both mTORC1 and mTORC2, but further research is warranted to clarify the distinct roles of mTORC1 and mTORC2 in cell motility. These results suggested that mTOR kinase inhibitors might be useful for the treatment of metastatic cancer, though this possibility needs to be tested in animal models and ultimately in the clinic.

In summary, we described the identification and characterization of a novel pyrazolopyrimidine-based mTOR kinase inhibitor X-387. X-387 possessed potent activity against cell proliferation and motility. X-387 also potently inhibited phosphorylation of AKT at T308 not via inhibition of PI3K. It further showed synergy in inhibition of cancer cell proliferation when combined with an inhibitor of autophagy. Thus, X-387 represents a promising compound lead targeting mTOR signaling and can be a useful tool in further elucidating the complex signaling pathways of mTOR.

Conflict of interest

C. Liang is cofounder and the chief scientific officer of Xcovery. The other authors disclosed no potential conflicts of interest.

Acknowledgments

This work was supported by National Science & Technology Major Project "Key New Drug Creation and Manufacturing Program" (2012ZX09301-001), National Natural Science Foundation of China (81021062, 81173079), Knowledge Innovation Program of Chinese Academy of Sciences (KSCX2-EW-Q-3). L.-H. Meng gratefully acknowledges the support of SA-SIBS Scholarship Program.

Appendix A. Supplementary data

Supplementary data associated with this article can be found, in the online version, at doi:10.1016/j.bcp.2012.01.019.

References

[1] Peterson TR, Laplante M, Thoreen CC, Sancak Y, Kang SA, Kuehl WM, et al. DEPTOR is an mTOR inhibitor frequently overexpressed in multiple myeloma cells and required for their survival. Cell 2009;137:873–86.
[2] Hara K, Maruki Y, Long XM, Yoshino K, Oshiro N, Hidayat S, et al. Raptor, a binding partner of target of rapamycin (TOR), mediates TOR action. Cell 2002;110:177–89.
[3] Sarbassov DD, Ali SM, Kim DH, Guertin DA, Latek RR, Erdjument-Bromage H, et al. Rictor, a novel binding partner of mTOR, defines a rapamycin-insensitive and raptor-independent pathway that regulates the cytoskeleton. Curr Biol 2004;14:1296–302.
[4] Ma XM, Blenis J. Molecular mechanisms of mTOR-mediated translational control. Nat Rev Mol Cell Biol 2009;10:307–18.
[5] Guertin DA, Stevens DM, Thoreen CC, Burds AA, Kalaany NY, Moffat J, et al. Ablation in mice of the mTORC components raptor, rictor, or mLST8 reveals that mTORC2 is required for signaling to Akt-FOXO and PKC alpha but not S6K1. Dev Cell 2006;11:859–71.
[6] De Benedetti A, Graff JR. eIF-4E expression and its role in malignancies and metastases. Oncogene 2004;23:3189–99.
[7] Nakamura JL, Garcia E, Pieper RO. S6K1 plays a key role in glial transformation. Cancer Res 2008;68:6516–23.
[8] Neshat MS, Mellinghoff IK, Tran C, Stiles B, Thomas G, Petersen R, et al. Enhanced sensitivity of PTEN-deficient tumors to inhibition of FRAP/mTOR. Proc Natl Acad Sci USA 2001;98:10314–9.
[9] Han S, Polizzano C, Nielsen GP, Hornicek FJ, Rosenberg AE, Ramesh V. Aberrant hyperactivation of akt and mammalian target of rapamycin complex 1 signaling in sporadic chordomas. Clin Cancer Res 2009;15:1940–6.
[10] Mavrommati I, Maffucci T. mTOR inhibitors: facing new challenges ahead. Curr Med Chem 2011;18:2743–62.
[11] Skehan P, Storeng R, Scudiero D, Monks A, McMahon J, Vistica D, et al. New colorimetric cytotoxicity assay for anticancer-drug screening. J Natl Cancer Inst 1990;82:1107–12.
[12] Volund A. Application of the four-parameter logistic model to bioassay: comparison with slope ratio and parallel line models. Biometrics 1978;34:357–65.
[13] Li T, Wang J, Wang X, Yang N, Chen SM, Tong LJ, et al. WJD008, a dual phosphatidylinositol 3-kinase (PI3K)/mammalian target of rapamycin inhibitor, prevents PI3K signaling and inhibits the proliferation of transformed cells with oncogenic PI3K mutant. J Pharmacol Exp Ther 2010;334:830–8.
[14] Yu K, Toral-Barza L, Shi C, Zhang WG, Lucas J, Shor B, et al. Biochemical, cellular, and in vivo activity of novel ATP-competitive and selective inhibitors of the mammalian target of rapamycin. Cancer Res 2009;69:6232–40.
[15] Ma JG, Huang H, Chen SM, Chen Y, Xin XL, Lin LP, et al. PH006, a novel and selective Src kinase inhibitor, suppresses human breast cancer growth and metastasis in vitro and in vivo. Breast Cancer Res Treat 2010.
[16] Zhang C, Yang N, Yang CH, Ding HS, Luo C, Zhang Y, et al. S9, a novel anticancer agent, exerts its anti-proliferative activity by interfering with both PI3K-Akt-mTOR signaling and microtubule cytoskeleton. PLoS ONE 2009;4:e4881.
[17] Ma JG, Huang H, Chen SM, Chen Y, Xin XL, Lin LP, et al. PH006, a novel and selective Src kinase inhibitor, suppresses human breast cancer growth and metastasis in vitro and in vivo. Breast Cancer Res Treat 2011;130:85–96.
[18] Su B, Jacinto E. Mammalian TOR signaling to the AGC kinases. Crit Rev Biochem Mol Biol 2011;46:527–47.
[19] Feldman ME, Apsel B, Uotila A, Loewith R, Knight ZA, Ruggero D, et al. Active-site inhibitors of mTOR target rapamycin-resistant outputs of mTORC1 and mTORC2. PLoS Biol 2009;7:e38.
[20] Burnett PE, Barrow RK, Cohen NA, Snyder SH, Sabatini DM. RAFT1 phosphorylation of the translational regulators p70 S6 kinase and 4E-BP1. Proc Natl Acad Sci USA 1998;95:1432–7.
[21] O'Reilly KE, Rojo F, She QB, Solit D, Mills GB, Smith D, et al. mTOR inhibition induces upstream receptor tyrosine kinase signaling and activates Akt. Cancer Res 2006;66:1500–8.
[22] Bhaskar PT, Hay N. The two TORCs and Akt. Dev Cell 2007;12:487–502.
[23] Soria JC, Shepherd FA, Douillard JY, Wolf J, Giaccone G, Crino L, et al. Efficacy of everolimus (RAD001) in patients with advanced NSCLC previously treated with chemotherapy alone or with chemotherapy and EGFR inhibitors. Ann Oncol 2009;20:1674–81.
[24] Dowling RJO, Topisirovic I, Alain T, Bidinosti M, Fonseca BD, Petroulakis E, et al. mTORC1-mediated cell proliferation, but not cell growth, controlled by the 4E-BPs. Science 2010;328:1172–6.
[25] Pattingre S, Espert L, Biard-Piechaczyk M, Codogno P. Regulation of macroautophagy by mTOR and Beclin 1 complexes. Biochimie 2008;90:313–23.
[26] Dalby KN, Tekedereli I, Lopez-Berestein G, Ozpolat B. Targeting the prodeath and prosurvival functions of autophagy as novel therapeutic strategies in cancer. Autophagy 2010;6:322–9.
[27] Moss SC, Lightell DJ, Marx SO, Marks AR, Woods TC. Rapamycin regulates endothelial cell migration through regulation of the cyclin-dependent kinase inhibitor p27(Kip1). J Biol Chem 2010;285:11991–7.
[28] Liu L, Luo Y, Chen L, Shen T, Xu B, Chen W, et al. Rapamycin inhibits cytoskeleton reorganization and cell motility by suppressing RhoA expression and activity. J Biol Chem 2010;285:38362–73.
[29] Liu L, Chen L, Luo Y, Chen W, Zhou H, Xu B, et al. Rapamycin inhibits IGF-1 stimulated cell motility through PP2A pathway. PLoS ONE 2010;5:e10578.
[30] Jacinto E, Loewith R, Schmidt A, Lin S, Ruegg MA, Hall A, et al. Mammalian TOR complex 2 controls the actin cytoskeleton and is rapamycin insensitive. Nat Cell Biol 2004;6:1122–30.
[31] Dos DS, Ali SM, Kim D-H, Guertin DA, Latek RR, Erdjument-Bromage H, et al. Rictor, a novel binding partner of mTOR, defines a rapamycin-insensitive and raptor-independent pathway that regulates the cytoskeleton. Curr Biol 2004;14:1296–302.
[32] Gulhati P, Bowen KA, Liu J, Stevens PD, Rychahou PG, Chen M, et al. mTORC1 and mTORC2 Regulate EMT, motility, and metastasis of colorectal cancer via RhoA and Rac1 signaling pathways. Cancer Res 2011;71:3246–56.

[33] Garcia-Martinez JM, Moran J, Clarke RG, Gray A, Cosulich SC, Chresta CM, et al. Ku-0063794 is a specific inhibitor of the mammalian target of rapamycin (mTOR). Biochem J 2009;421:29–42.
[34] Balsara BR, Pei J, Mitsuuchi Y, Page R, Klein-Szanto A, Wang H, et al. Frequent activation of AKT in non-small cell lung carcinomas and preneoplastic bronchial lesions. Carcinogenesis 2004;25:2053–9.
[35] Molina JRM, Sumithra J, Rowland K, Reuter NF, Jett JR, Marks R, et al. A phase II NCCTG window of opportunity front-line study of the mTOR Inhibitor, CCI-779 (Temsirolimus) given as a single agent in patients with advanced NSCLC: D7-07. J Thoracic Oncol 2007;2:S413.
[36] Yu L, McPhee CK, Zheng LX, Mardones GA, Rong YG, Peng JY, et al. Termination of autophagy and reformation of lysosomes regulated by mTOR. Nature 2010;465:942–1011.
[37] Levine B, Kroemer G. Autophagy in the pathogenesis of disease. Cell 2008;132:27–42.
[38] Mathew R, Karantza-Wadsworth V, White E. Role of autophagy in cancer. Nat Rev Cancer 2007;7:961–7.
[39] Yang Z, Klionsky DJ. Mammalian autophagy: core molecular machinery and signaling regulation. Curr Opin Cell Biol 2010;22:124–31.
[40] Mirzoeva OK, Hann B, Hom YK, Debnath J, Aftab D, Shokat K, et al. Autophagy suppression promotes apoptotic cell death in response to inhibition of the PI3K-mTOR pathway in pancreatic adenocarcinoma. J Mol Med (Berl) 2011;89:877–89.
[41] Huang S, Yang ZJ, Yu C, Sinicrope FA. Inhibition of mTOR kinase by AZD8055 can antagonize chemotherapy-induced cell death through autophagy induction and downregulation of p62/sequestosome 1. J Biol Chem 2011;286:40002–1.